8-1993

# Characterization of a Resistive Half Plane over a Resistive Sheet

John R. Natzke
*George Fox University*, jnatzke@georgefox.edu

John L. Volakis

# Characterization of a Resistive Half Plane over a Resistive Sheet

John R. Natzke, *Student Member, IEEE,* and John L. Volakis, *Senior Member, IEEE*

*Abstract*— **The diffraction of a resistive half plane over a planar resistive sheet under plane wave illumination is determined via the dual integral equation method (a variation of the Wiener–Hopf method). The solution is obtained upon splitting the associated Wiener–Hopf functions via a numerically efficient routine. Based on the derived exact half plane diffraction coefficient, a simplified equivalent model of the structure is developed when the separation of the half plane and resistive plane is on the order of a tenth of a wavelength or less. The model preserves the geometrical optics field of the original structure for all angles and is based on an approximate image theory of the resistive plane. Good agreement is obtained with the diffracted field exact solution.**

## I. Introduction

THE angular spectrum method set forth by Booker and Clemmow [1] has been applied to many diffracting structures composed of a half plane over a substrate [2]–[5]. In many cases resistive sheets [6] are used over dielectric layers for radar cross section control, transmittivity control, or other applications. Also, when the dielectric layer is thin, it can be equivalently replaced by a resistive sheet.

In this paper we particularly consider the diffraction by a resistive half plane vertically displaced from a uniform resistive sheet (see Fig. 1). The corresponding exact diffraction coefficient is derived for this configuration with an $H$-polarized illumination using the dual integral equation method, following a development similar to that in [3], [4]. The encountered Wiener–Hopf split function is factorized via an efficient numerical procedure discussed in [7].

When the separation between the resistive half plane and resistive sheet is on the order of a tenth of a wavelength or less, the structure is virtually planar. Thus a simplified model of the original configuration is a single equivalent resistive half plane illuminated by a direct and an image wave. This model relies on image theory to remove the lower planar sheet by introducing an image field and a second half plane placed symmetrically below the original resistive sheet. The two half planes are then combined into a single one with an equivalent resistivity such that the geometrical optics field of the original structure is preserved everywhere. The diffraction coefficient for this equivalent half plane is much simpler and is given by [8]. Several patterns are presented for assessing the model's accuracy for various resistivities and separation distances. This is done by comparison with the exact solution, which is in turn validated using a moment method solution.

Manuscript received August 18, 1992; revised March 19, 1993.

The authors are with the Department of Electrical Engineering and Computer Science, University of Michigan, Ann Arbor, MI 48109.

IEEE Log Number 9211793.

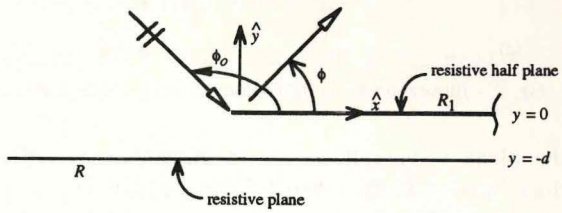


Fig. 1. Geometry of the resistive half plane over an infinite resistive sheet.

## II. Dual Integral Equation Formulation

Consider a resistive half plane of resistivity $R_1$, placed a distance $d$ above a planar resistive sheet of resistivity $R$ as shown in Fig. 1. Mathematically, the resistive half plane and the uniform resistive sheet satisfy the boundary conditions:

$$\hat{y} \times \hat{y} \times \boldsymbol{E} = -R_1 \hat{y} \times [\boldsymbol{H}^+ - \boldsymbol{H}^-] \qquad y = 0, \quad x > 0 \quad (1)$$

$$\hat{y} \times \hat{y} \times \boldsymbol{E} = -R \hat{y} \times [\boldsymbol{H}^+ - \boldsymbol{H}^-] \qquad y = -d, \quad -\infty < x < \infty, \quad (2)$$

in which $\boldsymbol{H}^{\pm}$ denotes the total magnetic field above and below the appropriate resistive sheet and $\boldsymbol{E}$ is likewise the total electric field, which is continuous across the sheets.

Assume the plane wave

$$\boldsymbol{H}^i = \hat{z} e^{jk\rho \cos(\phi - \phi_0)} \quad (3)$$

is impinging upon the structure in Fig. 1, where $k$ is the wave number, $(\rho, \phi)$ is the usual cylindrical coordinates, and $\phi_0$ is the angle of incidence such that $0 < \phi_0 < \pi$. For this excitation the total field may be represented as

$$H_z = \begin{cases} H_z^i + H_z^r + H_z^s, & y > -d \\ H_z^t + H_z^s, & y < -d. \end{cases} \quad (4)$$

We identify $H_z^r$ and $H_z^t$ as the reflected and transmitted fields, respectively, of the planar resistive sheet satisfying (2). Namely

$$H_z^r = -\Gamma(\sin\phi_0) e^{-j2kd \sin\phi_0} e^{jk\rho \cos(\phi + \phi_0)} \quad (5)$$

$$H_z^t = T(\sin\phi_0) e^{jk\rho \cos(\phi - \phi_0)}, \quad (6)$$

where

$$\Gamma(\sin\phi_0) = -\frac{\sin\phi_0}{\eta + \sin\phi_0},$$
$$T(\sin\phi_0) = 1 + \Gamma(\sin\phi_0) \quad (7)$$

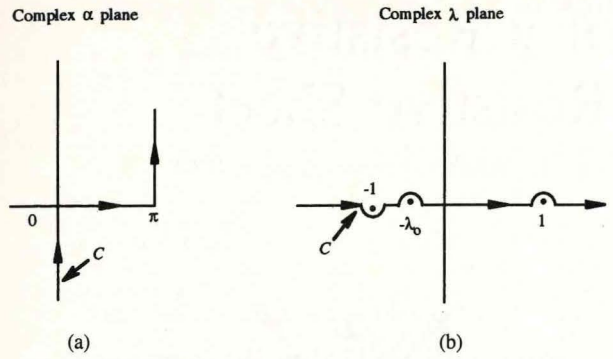


Fig. 2. Illustration of the $C$ contour in the $\alpha$ and $\lambda$ planes.

are the plane wave reflection and transmission coefficients in which $\eta = 2R/Z_0$. Further, we identify $H_z^s$ in (4) as the scattered field caused by the presence of the half plane at $y = 0$. This field is due to currents excited on the half plane which can be represented by an angular spectral integral [9]. Accounting for the reflections from (and transmissions through) the resistive plane at $y = -d$, the total scattered field is given by [3]

$$H_z^s = \int_C [1 + \Gamma(\sin\alpha)e^{-j2kd\sin\alpha}] \cdot P(\cos\alpha)e^{-jk\rho\cos(\phi-\alpha)}\,d\alpha \quad (8)$$

for $y > 0$,

$$H_z^s = -\int_C [e^{-jk\rho\cos(\phi+\alpha)} - \Gamma(\sin\alpha)e^{-j2kd\sin\alpha}e^{-jk\rho\cos(\phi-\alpha)}] \cdot P(\cos\alpha)\,d\alpha \quad (9)$$

for $-d < y < 0$, and

$$H_z^s = -\int_C T(\sin\alpha)P(\cos\alpha)e^{-jk\rho\cos(\phi+\alpha)}\,d\alpha \quad (10)$$

for $y < -d$, where the contour $C$ is defined in Fig. 2(a) and $P(\cos\alpha)$ is the unknown spectra proportional to the current on the half plane.

In the following we shall invoke the appropriate boundary conditions to determine the unknown spectra $P(\cos\alpha)$. First, to maintain the continuity of the total magnetic field across $x < 0$, $y = 0$, the condition $\hat{y} \times (\boldsymbol{H}^+ - \boldsymbol{H}^-) = 0$ must be satisfied. Upon using (3), (5), (8), and (9) in conjunction with (4), this condition implies

$$\int_{-\infty}^{\infty} \frac{P(\lambda)}{\sqrt{1-\lambda^2}} e^{-jkx\lambda}\,d\lambda = 0, \qquad x < 0, \quad (11)$$

where $\lambda = \cos\alpha$, and the path of integration is shown in Fig. 2(b). Since this integral equation is valid only for $x < 0$, the path of integration can be closed by a semi-infinite circle in the upper $\lambda$ plane without altering the result of the integration. From Cauchy's theorem, $P(\lambda)/\sqrt{1-\lambda^2}$ must then be free of zeros, branch cuts, or any other singularities in the upper half plane. Consequently, we can state that

$$\frac{P(\lambda)}{\sqrt{1-\lambda^2}} = U(\lambda), \quad (12)$$

where $U(\lambda)$ is a function regular in the upper half of the $\lambda$ plane.

The application of (1) across the half plane $x > 0$, $y = 0$, leads to the integral equation

$$\int_{-\infty}^{\infty} \left[\frac{\eta_1}{\sqrt{1-\lambda^2}} + 1 + \Gamma(\sqrt{1-\lambda^2})e^{-j2kd\sqrt{1-\lambda^2}}\right] \cdot P(\lambda)e^{-jkx\lambda}\,d\lambda = \sqrt{1-\lambda_0^2}\left[1 + \Gamma(\sqrt{1-\lambda_0^2})e^{-j2kd\sqrt{1-\lambda_0^2}}\right]e^{jkx\lambda_0}, \quad x > 0, \quad (13)$$

in which $\eta_1 = 2R_1/Z_0$ and $\lambda_0 = \cos\phi_0$. Since (13) is valid only for $x > 0$, the path of integration may now be closed by a semi-infinite circle in the lower half of the $\lambda$ plane. On applying Cauchy's theorem we then obtain the functional equation

$$Q(\lambda)\frac{P(\lambda)}{\sqrt{1-\lambda^2}} = -\frac{1}{2\pi j}\frac{L(\lambda)}{L(-\lambda_0)}\frac{\sqrt{1-\lambda_0^2}}{\lambda+\lambda_0}A(\sqrt{1-\lambda_0^2}) \quad (14)$$

where

$$Q(\lambda) = \eta_1 + \sqrt{1-\lambda^2}[1 + \Gamma(\sqrt{1-\lambda^2})e^{-j2kd\sqrt{1-\lambda^2}}], \quad (15)$$

$$A(\sqrt{1-\lambda_0^2}) = 1 + \Gamma(\sqrt{1-\lambda_0^2})e^{-j2kd\sqrt{1-\lambda_0^2}}, \quad (16)$$

and $L(\lambda)$ is a function regular in the lower half of the $\lambda$ plane.

To proceed further, $Q(\lambda)$ must first be factorized as a product of upper and lower half plane functions. In light of (7), we write (15) as

$$Q(\lambda) = \frac{U_w(\lambda)L_w(\lambda)}{U_s(\lambda)L_s(\lambda)}, \quad (17)$$

where

$$U_w(\lambda)L_w(\lambda) = (\eta_1 + \sqrt{1-\lambda^2})(\eta + \sqrt{1-\lambda^2}) - (1-\lambda^2)e^{-j2kd\sqrt{1-\lambda^2}} \quad (18)$$

and

$$U_s(\lambda)L_s(\lambda) = \eta + \sqrt{1-\lambda^2}. \quad (19)$$

Here $U_w(\lambda)$ and $U_s(\lambda)$ denote upper half plane functions and $L_w(\lambda)$ and $L_s(\lambda)$ denote lower half plane functions. The factorization of (18) can be accomplished using numerical methods [7]. For the case of (19), the known factorization [10]

$$\left(\gamma + \frac{1}{\sqrt{1-\lambda^2}}\right)^{-1} = K_+(\lambda,\gamma)K_-(\lambda,\gamma) \quad (20)$$

is noted, resulting in

$$U_s(\lambda) = \sqrt{\eta}\frac{\sqrt{1-\lambda}}{K_+(\lambda, 1/\eta)} = L_s(-\lambda). \quad (21)$$

Explicit, nonintegral expressions for $K_+(\lambda,\gamma)$ are given in [11] for $\mathrm{Re}(\gamma) > 0$. If $\mathrm{Re}(\gamma) < 0$, then $K_+(\lambda,\gamma)$ must be replaced with the expression [12]

$$j\frac{1}{\gamma}\frac{\lambda - \sqrt{1-\gamma^2}}{K_+(\lambda,-\gamma)}.$$

Returning now to (14), upon making use of (17) and (12), we find that $L(\lambda) = L_w(\lambda)/L_s(\lambda)$ to ensure the regularity

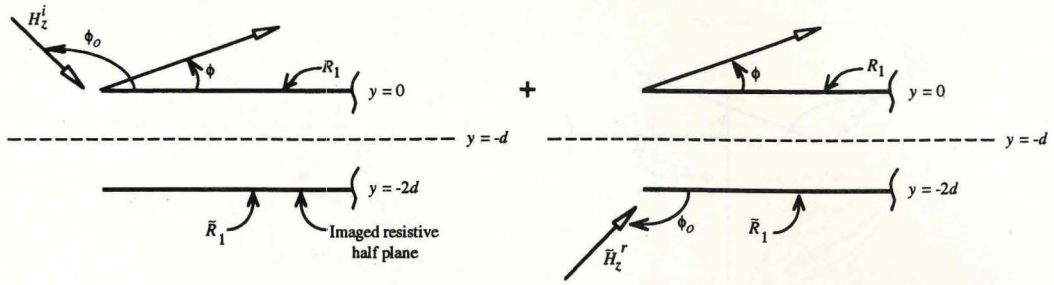


Fig. 3. Intermediate equivalent geometry problem recovering the GO field ($y > 0$) of the structure in Fig. 1.

of $U(\lambda)$ and $L(\lambda)$ in their respective planes. Then from (14) we obtain

$$P(\lambda) = -\frac{1}{2\pi j}\frac{\sqrt{1-\lambda^2}\sqrt{1-\lambda_0^2}}{\lambda+\lambda_0}A(\sqrt{1-\lambda_0^2}) \cdot\frac{U_s(\lambda)}{U_w(\lambda)}\frac{L_s(-\lambda_0)}{L_w(-\lambda_0)}. \quad (22)$$

This is proportional to the spectrum of the current on the resistive half plane in the presence of the resistive sheet at $y = -d$.

The far-zone scattered field is determined by substituting the spectral function $P(\lambda)$ as given by (22) into (8) and (10) and evaluating the integrals via the steepest descent method. Doing so, we obtain the form

$$H_z^s \simeq \frac{e^{-jk\rho}}{\sqrt{\rho}}S_1(\phi, \phi_0),$$

where $S_1(\phi, \phi_0)$ is often denoted as the diffraction coefficient of the configuration and is given by

$$S_1(\phi, \phi_0) = -\frac{e^{-j\pi/4}}{\sqrt{2\pi k}}\left\{\begin{matrix} A(\sin\phi) \\ T(-\sin\phi)\end{matrix}\right\} \cdot A(\sin\phi_0)\frac{\sin\phi\sin\phi_0}{\cos\phi+\cos\phi_0} \cdot\frac{U_s(\cos\phi)U_s(\cos\phi_0)}{U_w(\cos\phi)U_w(\cos\phi_0)} \quad (23)$$

$$\text{for} \quad \left\{\begin{matrix} 0<\phi<\pi \\ \pi<\phi<2\pi\end{matrix}\right\}.$$

In deriving this expression the identities $U_s(\lambda) = L_s(-\lambda)$ and $U_w(\lambda) = L_w(-\lambda)$ were employed. $S_1(\phi, \phi_0)$ is generally referred to as the diffraction coefficient of the upper resistive half plane in the presence of the lower sheet.

The diffracted field expressions can be verified for two limiting cases. When $\eta \to \infty$, the resistive sheet vanishes, and the diffraction coefficient becomes

$$S_1(\phi, \phi_0) = D_H(\phi, \phi_0, \eta_1) = -\frac{2e^{-j\pi/4}}{\eta_1\sqrt{2\pi k}}\frac{\cos\frac{\phi}{2}\cos\frac{\phi_0}{2}}{\cos\phi+\cos\phi_0} \cdot K_+(\cos\phi, 1/\eta_1)K_+(\cos\phi_0, 1/\eta_1) \quad (24)$$

as given in [8]. The other limiting case is $d \to 0$, for which (23) reduces to the $H$-polarization diffraction coefficient of a junction formed by two coplanar resistive half planes as derived in [13]. The pertinent half planes have resistivities $R = 2Z_0/\eta$ ($x < 0$) and $R_2 = 2Z_0/\eta_2$ ($x > 0$), where $\eta_2 = \eta_1\eta/(\eta_1+\eta)$.

## III. Simplified Model for Small $d$

When the separation between the resistive half plane and lower resistive sheet is small (i.e., $kd \ll 1$), the structure is virtually planar, and it is possible and instructive to seek a simplification of the exact solution developed in the previous section. To do so we shall first construct an equivalent geometry which recovers the geometrical optics (GO) fields of the original one in Fig. 1. With this in mind, $R$ can be removed by introducing an appropriate image of the resistive half plane and of the incident field as illustrated in Fig. 3. To recover the GO fields of the original geometry it is necessary to sum the GO fields associated with the pair of half planes in Fig. 3 under the direct ($H_z^i$) and imaged ($\tilde{H}_z^r$) illumination. In addition, an appropriate value for the resistivity $\tilde{R}_1$ of the imaged half plane must be specified. To determine $\tilde{R}_1$ and $\tilde{H}_z^r$ we consider the GO fields of the original structure. The reflected field associated with its right side (side of the resistive half plane) is found to be

$$H_z^{r1} = -\left[\Gamma_1 + \frac{T_1^2\Gamma e^{-j2kd\sin\phi_0}}{1-\Gamma_1\Gamma e^{-j2kd\sin\phi_0}}\right]e^{jk\rho\cos(\phi+\phi_0)}, \quad y > 0, \quad (25)$$

where $\Gamma$ and $T$ are defined in (7) and

$$\Gamma_1 = -\frac{\sin\phi_0}{\eta_1+\sin\phi_0} \qquad T_1 = \frac{\eta_1}{\eta_1+\sin\phi_0} \quad (26)$$

with $\eta_1 = 2R_1/Z_0$. The appropriate reflected field for the left side of the same geometry can be obtained by letting $\eta_1 \to \infty$. On comparing the sum of the GO fields generated by the pair of sheets in Fig. 3 under the two illuminations with (25), we deduce that

$$\tilde{R}_1 = -\frac{Z_0}{2}\sin\phi_0\frac{1+\Gamma_1\Gamma^2}{\Gamma_1\Gamma^2}$$

and

$$\tilde{H}_z^r = \begin{cases}\tilde{\Gamma}H_z^r & \phi < \pi-\phi_0 \\ H_z^r & \phi > \pi-\phi_0,\end{cases}$$

in which

$$\tilde{\Gamma} = \frac{T_1}{1+\Gamma_1\Gamma^2}$$

and $H_z^r$ is given in (5). Note that $\tilde{R}_1$ and $\tilde{\Gamma}$ are functions of the incidence angle since our requirement was to recover the GO fields of the original structure for all incidence angles.

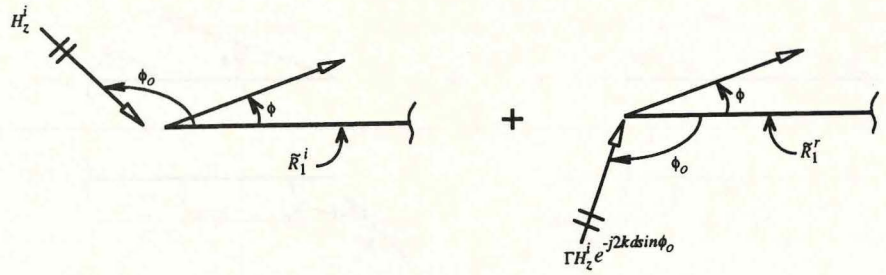


Fig. 4. Equivalent set of single resistive half planes recovering the reflected GO field ($y > 0$) of the structure in Fig. 1. The half planes lie in the $y = -d$ plane.

Having determined the resistivity of the imaged half plane $\tilde{R}_1$, we now proceed to combine the pair of half planes into a single equivalent half plane at $x > 0$, $y = -q$, $0 \le q \le d$. This is illustrated in Fig. 4 and for each illumination a different resistivity is required. This can be determined by comparing the GO fields (reflected for the direct illumination and transmitted for the imaged illumination) of the configurations in Figs. 3 and 4 and requiring that they be equal. Doing so, we find that the resistivity of the single equivalent half plane subjected to direct illumination must be

$$\tilde{R}_1^i = -\frac{Z_0}{2}\sin\phi_0 \frac{1+\tilde{\Gamma}_1^i}{\tilde{\Gamma}_1^i} \tag{27}$$

where

$$\tilde{\Gamma}_1^i = \Gamma_1\left[1 + \frac{T_1^2\Gamma^2 e^{-j4kd\sin\phi_0}}{1-\Gamma_1^2\Gamma^2 e^{-j4kd\sin\phi_0}}\right] e^{j2kq\sin\phi_0}. \tag{28}$$

When $q = 0$, the equivalent half plane is coincident with the original resistive half plane, and the equivalent resistivity $\tilde{R}_1^i$ was seen to have an average value of $R_1$ as $d$ was varied. Based on this observation and accounting for the $\phi_0$ dependence, an excellent approximation to $\tilde{R}_1^i$ for all $q$, $0 \le q \le d$, is found to be

$$\tilde{R}_1^i \simeq [R_1 - (R_1 - \tilde{R}_2)e^{-j4kd\sin\phi_0}]e^{-j2kq\sin\phi_0} + \frac{Z_0}{2}\sin\phi_0(e^{-j2kq\sin\phi_0} - 1), \tag{29}$$

where

$$\tilde{R}_2 = \frac{R_1\tilde{R}_1}{R_1 + \tilde{R}_1},$$

which is the same as (27) and (28) with $d = 0$. We determined that for far-field scattering the best results were obtained by setting $q = d$. That is, the accuracy of the model was not adequate when $\tilde{R}_1^i$ is replaced by its average value of $R_1$. It is therefore necessary to retain the more accurate expressions for $\tilde{R}_1^i$ given by (27) or (29), which are, unfortunately, functions of the incidence angle.

For the imaged illumination, the corresponding half plane resistivity is found to be

$$\tilde{R}_1^r = \frac{Z_0}{2}\sin\phi_0\frac{\tilde{T}_1^r}{1-\tilde{T}_1^r} \tag{30}$$

with

$$\tilde{T}_1^r = \frac{T_1^2}{1-\Gamma_1^2\Gamma^2 e^{-j4kd\sin\phi_0}} \tag{31}$$

and the associated imaged field being set to $H_z^r$, $0 < \phi < \pi$. With this imaged field, the reflected field of Fig. 4(a) plus the transmitted field of Fig. 4(b) completely recover the GO field of the original configuration in the entire $y > 0$ region. Equations (30) and (31) show that $\tilde{R}_1^r \le R_1/2$ as $d$ and $\phi_0$ are varied, although its average value is not a constant. We found, however, that if $R_1 \lesssim R$, the variation of $\tilde{R}_1^r$ with $d$ and $\phi_0$ is sufficiently small such that a good approximation is the constant

$$\tilde{R}_1^r \simeq \frac{Z_0}{2}\frac{\eta_1^2(\eta+1)^2}{(2\eta_1+1)(\eta+1)^2-1}, \tag{32}$$

which is the expression reduced from (30) and (31) on setting $d = 0$ and $\phi_0 = \pi/2$.

The far-zone diffracted field as predicted by the single half plane models of Fig. 4 is easily computed by using the diffraction coefficient (24). In particular, on superposing the fields generated by the direct and imaged illumination, we obtain the composite diffraction coefficient

$$S_2(\phi, \phi_0) = [D_H(\phi, \phi_0, \tilde{\eta}_1^i) - \Gamma(\sin\phi_0)D_H(\phi, 2\pi-\phi_0, \tilde{\eta}_1^r)] \cdot e^{-jkd(\sin\phi+\sin\phi_0)}, \quad 0 < \phi < \pi, \tag{33}$$

where $\tilde{\eta}_1^i = 2\tilde{R}_1^i/Z_0$ with $q = d$, $\tilde{\eta}_1^r = 2\tilde{R}_1^r/Z_0$, and $D_H$ is given in (24). This should be compared with the exact diffraction coefficient given in (23).

In the above, we presented a simplified equivalent model which recovers the reflected GO field of the original configuration in Fig. 1. It is not therefore expected that the same resistivities and associated model will also recover the transmitted GO field through the same configuration. Nevertheless, a similar procedure can be employed to construct an equivalent problem which is associated with the same GO field in the $y < 0$ region. Such a model is illustrated in Fig. 5, and in order for this model to recover the same GO transmitted field as that associated with the configuration in Fig. 1 we find that the resistivity of the equivalent half plane must be

$$\tilde{R}_1^t = \frac{Z_0}{2}\sin\phi_0\frac{\tilde{T}_1^t}{1-\tilde{T}_1^t}, \tag{34}$$

where

$$\tilde{T}_1^t = \frac{T_1}{1-\Gamma_1\Gamma e^{-j2kd\sin\phi_0}}. \tag{35}$$

The corresponding diffracted field is given by

$$S_2(\phi, \phi_0) = T(\sin\phi_0)D_H(\phi, \phi_0, \tilde{\eta}_1^t)e^{-jkd(\sin\phi+\sin\phi_0)}, \tag{36}$$

where $\pi < \phi < 2\pi$ and as usual $\tilde{\eta}_1^t = 2\tilde{R}_1^t/Z_0$. This diffraction coefficient should be compared with the exact one given by (23).

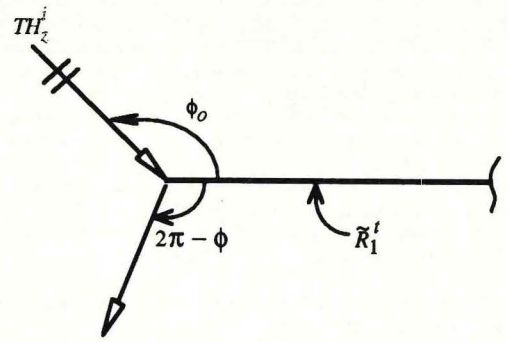


Fig. 5. Equivalent problem recovering the transmitted GO field ($y < -d$) of the structure in Fig. 1.

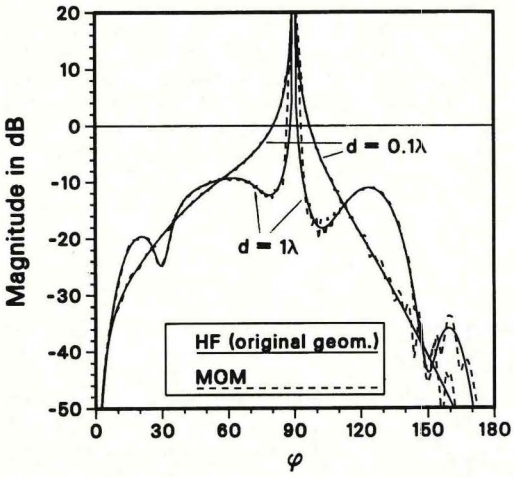


Fig. 6. Comparison of backscatter as computed by the moment method and high-frequency solutions (of the exact geometry) of the resistive half plane configuration in Fig. 1 with $R = R_1 = Z_0/4$ for $d = 0.1\lambda$ and $d = 1\lambda$.

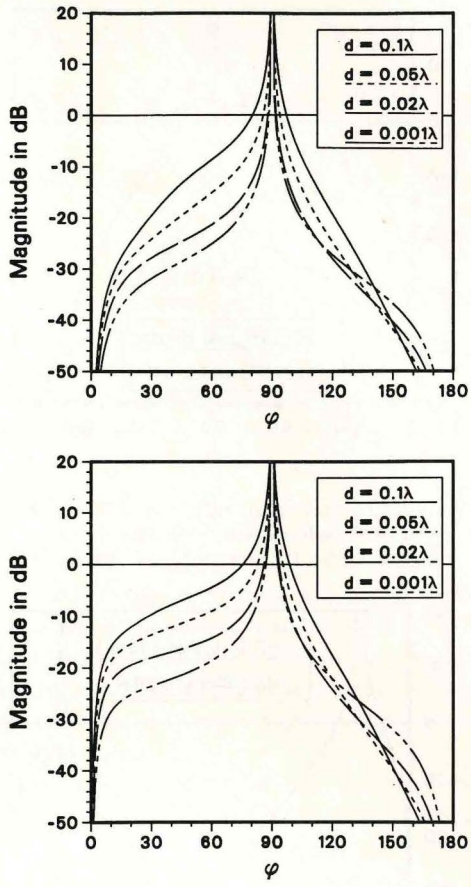


Fig. 7. Family of backscatter RCS curves (using the original geometry high-frequency solution) of the half plane configuration in Fig. 1 for different separation distances $d$. $R = R_1 = Z_0/4$ (top); $R = Z_0/4$, $R_1 = Z_0/20$ (bottom).

## IV. Numerical Results

The far-field amplitude $S_1(\phi, \phi_0)$ in (23) was programmed for solution. The numerical factorization routine [7] was used to determine the upper half plane function $U_w$. As part of the verification of $S_1(\phi, \phi_0)$, the limit as $R \to \infty$ was taken and the result converged to that of an isolated resistive half plane $R_1$ as given in (24). Also, by taking the limit $d \to 0$, $S_1(\phi, \phi_0)$ was found to be in agreement with the material junction result in [13]. To complete the verification, the RCS based on the derived diffraction coefficient $S_1(\phi, \phi_0)$ was compared with data generated by a method of moments implementation of the resistive half plane over resistive plane structure. RCS backscatter results are shown in Fig. 6 for separations of $d = 0.1\lambda$ and $1.0\lambda$ with $R = R_1 = Z_0/4$. The moment method data were generated by replacing the resistive half plane and infinite sheet with very wide resistive strips whose resistivity profile after being equal to either $R$ or $R_1$ was then tapered quadratically to $20Z_0$ over a $60\lambda$ section. As seen, the agreement between the numerical and high-frequency solutions is excellent. Having validated the high-frequency solution, Fig. 7 then shows a characterization of the resistive half plane over the resistive sheet for different separation distances ranging from $d = 0.001\lambda$ to $d = 0.1\lambda$.

To test the validity of the proposed simplified model (see Figs. 4 and 5), the far-field amplitudes $S_2(\phi, \phi_0)$ in (33) and (36) were programmed as well. Backscatter results in magnitude are shown in Fig. 8 for $d = 0.01\lambda$ with $R = R_1 = Z_0/4$ and for $d = 0.25\lambda$ with $R = Z_0/4$, $R_1 = Z_0/20$. Good agreement is obtained between the magnitudes of the high-frequency solutions based on the original and simplified geometries for all angles $\phi$, and $d \simeq 0.25\lambda$ was found to be the upper limit of the half plane model. This also holds for bistatic computations except near grazing angles of observation for some values of $d$. An example of a bistatic pattern is shown in Fig. 9, and it is again verified that the simplified model is a good representation of the original geometry.

## V. Summary

The exact diffraction coefficient was derived for a resistive half plane over an infinite resistive sheet using the dual integral equation method. An efficient numerical routine was employed to factorize the associated Wiener–Hopf split function. The high-frequency solution was found to be in excellent agreement with data generated by a method of moments implementation of the structure, and the results were also verified for the two limiting cases (in the absence of the infinite resistive sheet and when the separation distance between the resistive half plane and sheet goes to zero).

Using the exact solution as a reference, a simplified equivalent model of the structure was developed for the case where

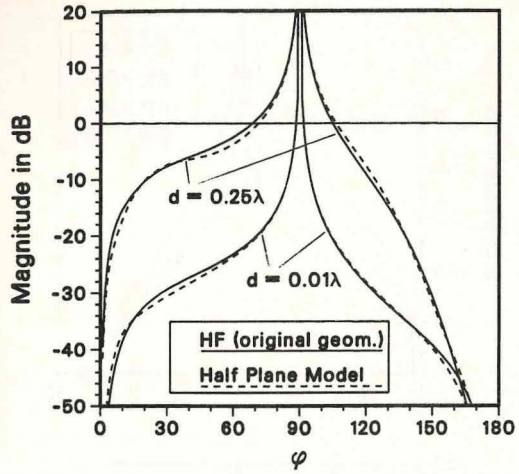


Fig. 8. Comparison of backscatter RCS curves based on the original geometry and simplified high-frequency solutions for $d = 0.01\lambda$ with $R = R_1 = Z_0/4$ and for $d = 0.25\lambda$ with $R = Z_0/4$, $R_1 = Z_0/20$.

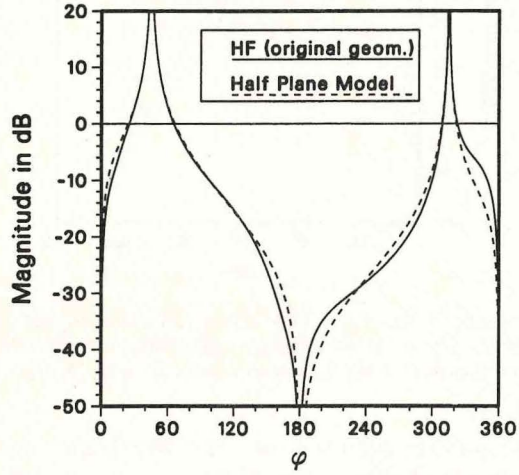


Fig. 9. Comparison of bistatic RCS curves based on the original geometry and simplified high-frequency solutions for $\phi_0 = 3\pi/4$, $R = R_1 = Z_0/4$, and $d = 0.25\lambda$.

the separation of the resistive half plane and sheet is on the order of a tenth of a wavelength or less. The model consisted of a single resistive half plane illuminated with a direct and an image wave equal to the reflected field of the infinite sheet. Good agreement was generally obtained between the high-frequency solutions based on the original geometry and the simplified equivalent model for separation distances of up to $d \simeq 0.25\lambda$.

## ACKNOWLEDGMENT

The authors are indebted to L. C. Kempel for his assistance in generating the moment method data reported in this paper.

## REFERENCES

[1] H. G. Booker and P. C. Clemmow, "The concept of an angular spectrum of plane waves and its relation to that of polar diagrams and aperture distribution," *Proc. Inst. Elect. Eng.*, vol. 97, pp. 11–17, 1950.

[2] P. C. Clemmow, "Radio propagation over a flat earth across a boundary separating two different media," *Phil. Trans. R. Soc. London., Ser. A*, vol. 246, pp. 1–55, 1953.

[3] Y. Sunahara and T. Sekiguchi, "Ray theory of diffraction by a half-sheet parallel to a flat earth," *Radio Sci.*, vol. 16, no. 1, pp. 141–155, 1981.

[4] M. A. Ricoy and J. L. Volakis, "Diffraction by a multilayer slab recessed in a ground plane via generalized impedance boundary conditions," *Radio Sci.*, vol. 26, no. 2, pp. 313–327, 1991.

[5] J. L. Volakis and J. D. Collins, "Electromagnetic scattering from a resistive half plane on a dielectric interface," *Wave Motion*, vol. 12, pp. 81–96, 1990.

[6] T. B. A. Senior, "Combined resistive and conductive sheets," *IEEE Trans. Antennas Propagat.*, vol. 33, pp. 577–579, 1985.

[7] M. A. Ricoy and J. L. Volakis, "*E*-polarization diffraction by a thick metal-dielectric join," *J. Electromagn. Waves Appl.*, vol. 3, pp. 383–407, 1989.

[8] T. B. A. Senior, "Half plane edge diffraction," *Radio Sci.*, vol. 10, no. 16, pp. 645–650, 1975.

[9] P. C. Clemmow, "A method for exact solution of a class of two dimensional diffraction problems," *Proc. Roy. Soc. A*, vol. 205, pp. 286–308, 1951.

[10] T. B. A. Senior, "Diffraction by a semi-infinite metallic sheet," *Proc. Roy. Soc. (London), A*, vol. 213 (1115), pp. 436–458, 1952.

[11] J. L. Volakis, "High frequency scattering by a thin material half plane and strip," *Radio Sci.*, vol. 23, no. 3, pp. 450–462, 1988.

[12] M. A. Ricoy and J. L. Volakis, "Diffraction by a symmetric material junction simulated with generalized sheet transition conditions," *IEEE Trans. Antennas Propagat.*, vol. 40, pp. 742–754, 1992.

[13] T. B. A. Senior, "Diffraction by a material junction," *Radiation Lab. Report* RL-880, U. of Michigan, Ann Arbor, MI, 1990.

**John R. Natzke** (S84) was born in Manilla, IA, in August 1963. He received the B.S.E.E. degree from Milwaukee School of Engineering in 1985 and the M.S.E.E. degree from Marquette University, Milwaukee, WI, in 1988. He is presently a Ph.D. candidate in electrical engineering at the University of Michigan, Ann Arbor. His research interests include electromagnetic theory, scattering problems, microwave engineering, and the numerical methods applied to these areas.

Mr. Natzke is a member of Eta Kappa Nu and an associate member of Sigma Xi.

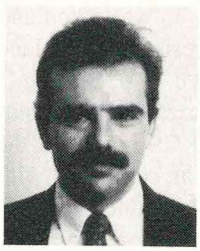

**John L. Volakis** (S'77–M'82–SM'89) was born on May 13, 1956, in Chios, Greece, where he also attended the Gymnasium of Males. He obtained the B.E. degree (summa cum laude) in 1978 from Youngstown State University, Youngstown, OH, the M.Sc. in 1979 from Ohio State University, Columbus, and the Ph.D. in 1982, also from Ohio State University.

He has been with the University of Michigan, Ann Arbor, since 1984, where he is now an Associate Professor in the Electrical Engineering and Computer Science (EECS) Department. From 1982 to 1984 he was with the Aircraft Division of Rockwell International and during the years 1978–1982 he was a Graduate Research Associate at the ElectroScience Laboratory, Ohio State University. His primary research interests are in the development of analytical and numerical techniques as applied to electromagnetics. In 1993 he received the University of Michigan EECS Department Research Excellence Award.

Dr. Volakis served in various posts of the local IEEE AP/MTT/ED Southeastern Michigan Chapter from 1985 to 1988 and was an Associated Editor of the IEEE TRANSACTIONS ON ANTENNAS AND PROPAGATION from 1988 to 1992. He is currently an Associate Editor for *Radio Science* and the *IEEE Antennas and Propagation Society Magazine*, and chaired the 1993 IEEE AP-S/URSI Symposium. He is a member of Sigma Xi, Tau Beta Pi, Phi Kappa Phi, and Commission B of URSI.